



HAL
open science

Comparisons among the five ground-motion models developed using RESORCE for the prediction of response spectral accelerations due to earthquakes in Europe and the Middle East

John Douglas, Sinan Akkar, Gabriele Ameri, Pierre-Yves Bard, Dino Bindi, Julian J. Bommer, Sanjay Singh Bora, Fabrice Cotton, Boumédiène Derras, Marcel Hermkes, et al.

► To cite this version:

John Douglas, Sinan Akkar, Gabriele Ameri, Pierre-Yves Bard, Dino Bindi, et al.. Comparisons among the five ground-motion models developed using RESORCE for the prediction of response spectral accelerations due to earthquakes in Europe and the Middle East. *Bulletin of Earthquake Engineering*, 2014, 12 (1), pp.341-358. 10.1007/s10518-013-9522-8 . hal-00862428

HAL Id: hal-00862428

<https://brgm.hal.science/hal-00862428v1>

Submitted on 16 Sep 2013

HAL is a multi-disciplinary open access archive for the deposit and dissemination of scientific research documents, whether they are published or not. The documents may come from teaching and research institutions in France or abroad, or from public or private research centers.

L'archive ouverte pluridisciplinaire **HAL**, est destinée au dépôt et à la diffusion de documents scientifiques de niveau recherche, publiés ou non, émanant des établissements d'enseignement et de recherche français ou étrangers, des laboratoires publics ou privés.

1 **Comparisons among the five ground-motion models developed using RESORCE for the**
2 **prediction of response spectral accelerations due to earthquakes in Europe and the Middle East**

3 John Douglas¹, Sinan Akkar², Gabriele Ameri³, Pierre-Yves Bard⁴, Dino Bindi⁵, Julian J. Bommer⁶,
4 Sanjay Singh Bora⁷, Fabrice Cotton⁴, Boumédiène Derras⁴, Marcel Hermkes⁷, Nicolas Martin Kuehn⁷,
5 Lucia Luzi⁸, Marco Massa⁸, Francesca Pacor⁸, Carsten Riggelsen⁷, M. Abdullah Sandikkaya²,
6 Frank Scherbaum⁷, Peter J. Stafford⁶, Paola Traversa⁹

7 *Abstract*

8 This article presents comparisons among the five ground-motion models described in other articles
9 within this special issue, in terms of data selection criteria, characteristics of the models and predicted
10 peak ground and response spectral accelerations. Comparisons are also made with predictions from the
11 Next Generation Attenuation (NGA) models to which the models presented here have similarities (e.g.
12 a common master database has been used) but also differences (e.g. some models in this issue are
13 nonparametric). As a result of the differing data selection criteria and derivation techniques the
14 predicted median ground motions show considerable differences (up to a factor of two for certain
15 scenarios), particularly for magnitudes and distances close to or beyond the range of the available
16 observations. The predicted influence of style-of-faulting shows much variation among models
17 whereas site amplification factors are more similar, with peak amplification at around 1s. These
18 differences are greater than those among predictions from the NGA models. The models for aleatory
19 variability (σ), however, are similar and suggest that ground-motion variability from this region is
20 slightly higher than that predicted by the NGA models, based primarily on data from California and
21 Taiwan.

22 *Keywords:* strong-motion data; ground-motion models; ground-motion prediction equations; style of
23 faulting; site amplification; aleatory variability; epistemic uncertainty; Europe; Middle East.

¹ BRGM, Orléans, France

² Middle East Technical University, Ankara, Turkey

³ FUGRO-Geoter, Auriol, France.

⁴ ISTERre, Université Joseph Fourier, CNRS, Grenoble, France

⁵ GFZ, Potsdam, Germany

⁶ Imperial College London, United Kingdom

⁷ Inst. Erd- und Umweltwissenschaften, Universitaet Potsdam, Germany

⁸ INGV, Milan, Italy

⁹ EDF, Aix en Provence, France

24 *1. Introduction*

25 The collection of five ground-motion models presented in other articles in this special issue has
26 similarities to the five sets of ground-motion prediction equations (GMPEs) derived during the Next
27 Generation Attenuation (NGA) project (Power *et al.*, 2008) and described in a special issue of
28 Earthquake Spectra in 2008. Firstly, both sets of models were derived for state-of-the-art seismic
29 hazard assessments for shallow active crustal seismicity in specific geographical regions: western
30 North America (specifically California) for NGA, and Europe and the Middle East here. In passing it
31 may be noted, however, that the NGA models have been shown to be applicable to Europe and the
32 Middle East (Stafford *et al.*, 2008). Secondly, all five GMPEs presented here were derived based on
33 records chosen from a common strong-motion database (RESORCE, see Akkar *et al.*, 2013c), whose
34 compilation has similarities to the procedure followed when developing the NGA database (Chiou *et al.*,
35 2008). Thirdly, careful data selections were made by each of the GMPE developers and state-of-
36 the-art derivation techniques were followed. Lastly, the collection of GMPEs produced seeks to
37 acknowledge the still considerable epistemic uncertainty present in the assessment of earthquake
38 shaking (e.g. Douglas, 2010). For the application of the NGA models within the USGS national hazard
39 calculations additional branches were added to the logic-tree in certain magnitude-distance bins to
40 capture epistemic uncertainty beyond that represented by these models (Petersen *et al.*, 2008).

41 On the other hand, the collection presents significant differences with respect to the NGA models.
42 Firstly, unlike the NGA models, which were all derived using regression analysis, generally the
43 random-effects approach (e.g. Abrahamson and Youngs, 1992), (although with some coefficients fixed
44 *a priori* based on physical arguments), here only two models were derived in this way (Akkar *et al.*,
45 2013a, b; Bindi *et al.*, 2013). Two of the others are non-parametric models derived using data-driven
46 approaches (Derras *et al.*, 2013; Hermkes *et al.*, 2013) and the other model (Bora *et al.*, 2013) makes
47 predictions of response spectral accelerations using random-vibration theory based on empirical
48 models for Fourier amplitude spectra and durations. Secondly, unlike the multi-year NGA project,
49 which involved extensive interactions among developers and other project participants (leading to
50 multiple iterations of the models), the models presented here were derived in a much shorter period
51 and following limited communication among groups. Although the development of RESORCE was
52 funded by SHARE and SIGMA, which led to some interactions among the model developers, this
53 special issue is principally the fruit of parallel and independent efforts (by authors in five countries)
54 rather than a coordinated national project. This means that the differences in the approaches used are
55 larger than for NGA. It is possible that the use of multiple approaches for the models presented in this
56 volume more effectively captures epistemic uncertainty in terms of the centre, the body and the range
57 of technically-defensible interpretations of the available data (USNRC, 2012). Thirdly, the
58 independent parameters used by the models presented here are: common among groups (all use only:

59 moment magnitude, M_w ; distance to the surface projection of the fault, R_{JB} ¹⁰; the same style-of-
60 faulting classifications; and the average shear-wave velocity to 30m, V_{S30}) and fewer (e.g. data were
61 insufficient to include terms involving sediment depth, $Z_{1.0}$ or $Z_{2.5}$, or depth to the top of rupture, Z_{TOR})
62 than in the NGA models. This makes comparisons among the models and their use in future seismic
63 hazard assessments easier since no adjustments for differences in independent parameters (e.g.
64 Bommer *et al.*, 2005) are required. Lastly, no strict model requirements were agreed at the beginning
65 of the derivation procedure, unlike those imposed on the NGA model developers, which means that
66 the models presented here have varying ranges of applicability in terms of, for example, magnitude
67 and distance.

68

69 Despite the differences between the NGA project and this special issue, the NGA comparison article
70 by Abrahamson *et al.* (2008) is used as a template for this article comparing the five models presented
71 in this issue, namely those by: Akkar *et al.* (2013a, b) (their model using R_{JB}), Bindi *et al.* (2013) (their
72 model using V_{S30} directly¹¹), Bora *et al.* (2013), Derras *et al.* (2013) and Hermkes *et al.* (2013). This
73 decision means that comparisons between the figures presented here can be readily made to those
74 shown in Abrahamson *et al.* (2008) because the same choices of independent parameters and the same
75 axes and scales are used (also to help in making these comparisons the same figure numbering has
76 been retained). Note that some of the graphs show predictions up to M_w 8, for consistency with
77 Abrahamson *et al.* (2008), even though some developers do not recommend their models are applied
78 for such large earthquakes (Table 1). To further facilitate comparisons with the NGA models,
79 predictions from the GMPEs of Boore and Atkinson (2008) are included on the figures. This NGA
80 model was chosen from among the five because it is the most similar to those presented in this special
81 issue through its use of R_{JB} and fewer independent variables, e.g. no terms using Z_{TOR} or $Z_{1.0}$ (or $Z_{2.5}$)
82 are included. Because the models presented here have fewer independent parameters and the aleatory
83 variabilities (standard deviations) of the models are all homoscedastic (uniform for all independent
84 and dependent variables) some figures drawn by Abrahamson *et al.* (2008) are not relevant and are not
85 drawn. They are replaced with figures showing other features of the models that are not covered by the
86 other graphs, for example the influence of style of faulting on ground-motion predictions (e.g.
87 Bommer *et al.*, 2003).

88

89 The next section presents the data selection criteria used by the different groups. The following
90 sections compare different aspects of the models in terms of: attenuation with distance, scaling with

¹⁰ Akkar *et al.* (2013a, b) also derived GMPEs using epicentral (R_{epi}) and hypocentral (R_{hyp}) distances. These are not considered in this article.

¹¹ Bindi *et al.* (2013) also derived GMPEs using hypocentral (R_{hyp}) distance and EC8 site classes rather than V_{S30} directly. These models are not considered in this article.

91 magnitude, style-of-faulting factors, site amplification, predicted response spectra and aleatory
92 variability. The article ends with some brief conclusions.

93 2. Data selection criteria

94 All GMPE developers started with the same RESORCE archive, which is presented by Akkar et al.
95 (2013a) in this special issue. At the time of model derivation this databank contained 5,882 mainly-
96 triaxial accelerograms (from $0 \leq R \leq 587 \text{ km}$) from 1,814 earthquakes (with $2.8 \leq M_w \leq 7.8$) and 1,540
97 different strong-motion stations. The five groups of developers applied different selection and
98 exclusion criteria, which led to them using between only 14% and 38% of the available accelerograms
99 (see Table 1). The same magnitude ranges were used by all groups, except by Derras *et al.* (2013) who
100 used a slightly lower minimum magnitude (3.6 rather than 4.0), to select their data and only Bindi *et*
101 *al.* (2013) and Derras *et al.* (2013) varied from the distance cut-off of 200km (using 300km and
102 547km, respectively, instead). None of the RESORCE developers used selection criteria based on
103 earthquake type (e.g. mainshock, aftershock or swarm) or considered its influence on ground motions.
104 Consequently all types of earthquakes (including aftershocks) were selected, unlike Boore and
105 Atkinson (2008) who exclude this type of event when deriving their NGA model and other NGA
106 models that included terms in their models to distinguish between mainshocks and aftershocks. As
107 discussed by Douglas and Halldorsson (2010) there is considerable doubt over the classification of
108 European earthquakes into mainshock, aftershock and swarm and their analysis using the data and
109 model of Ambraseys et al. (2005) suggested that the influence of earthquake type on ground motions
110 is limited. A similar conclusion is reached by Bindi et al. (2013) after examining the residuals for their
111 model separated into mainshock and aftershock classes. The five model databases principally
112 comprise records from normal and strike-slip earthquakes, with a smaller number of accelerograms
113 from reverse-faulting events. The distribution of records by style-of-faulting is reasonably uniform
114 with respect to magnitude but the largest ($M_w > 7$) earthquakes are mainly from strike-slip earthquakes
115 in Turkey (Kocaeli and Düzce) and Iran (Manjil). The variation in the final databases principally
116 results from the exclusion of data based on the filters used to process the accelerograms. The result of
117 these various selection criteria are different sizes of databases used for the derivations of the five
118 models (Table 1). All of the models were derived using roughly 1 000 strong-motion records.

119 One major difference between the data used by the models compared here and that used for the NGA
120 models is the large number of poorly-recorded earthquakes. This is indicated by the mean number of
121 records per earthquake for the five RESORCE models being between 3.0 and 5.8 (Table 1) whereas
122 the mean number of records per earthquake for the NGA models varies between 13.1 and 27.1. This
123 difference implies that the terms of the models related to the earthquake source (e.g. style-of-faulting
124 terms and between-event standard deviations) are more poorly constrained than they are in the NGA
125 models, which, as shown below, leads to significant differences in these aspects of the models. The

126 complexity of the source modelling in some of the NGA models, however, means that these models
127 may suffer from trade-offs, for example between the effect of Z_{TOR} and style-of-faulting.

128 3. Attenuation with distance

129 The decay with distance from the source for peak ground acceleration (PGA) and spectral acceleration
130 for a structural period of 1s and 5% critical damping [SA(1s)] can be seen in Figure 1, for
131 $V_{S30}=760\text{m/s}$, i.e. NEHRP B/C boundary (Building Seismic Safety Council, 2009) (soft rock,
132 Eurocode 8 class B), and in Figure 2, for $V_{S30}=270\text{m/s}$, i.e. NEHRP D (soft soil, Eurocode 8 class C).
133 Generally the decay rates are similar as are the predicted ground motions, particularly for small and
134 moderate events and PGA. Predictions from the models derived by standard regression techniques
135 (Akkar *et al.*, 2013a, b; Bindi *et al.*, 2013) are comparable except at the limits of their applicability
136 (M_w 8 and close to the source of large earthquakes, $R_{JB}<10\text{km}$). Bindi *et al.* (2013) include an anelastic
137 attenuation¹² term for short periods whereas Akkar *et al.* (2013a, b) tried including such a term but
138 found that it converged to a non-physical value and hence they removed it from their functional form.
139 Predictions from the nonparametric models show considerable variations and the model of Hermkes *et al.*
140 (2013) shows a complex decay rate, with a change of slope (often flattening) starting around 50km.
141 Despite all models having being derived from a common original archive (even if the final databases
142 used differed), a factor of two difference in predicted median ground motions from the models is not
143 uncommon, except for magnitudes and distance near the centre of the available data (e.g. M_w 6).

144 As is becoming commonly recognised and modelled, the decay of earthquake ground motions is
145 magnitude dependent. This effect can be seen by comparing the decay rates for M_w 5 (roughly $1/R^{1.5}$
146 for PGA) to those for M_w 8 (slower than $1/R$). The predicted ground motions from the RESORCE
147 models all decay more rapidly than those from the GMPEs of Boore and Atkinson (2008), particularly
148 for PGA, which leads to much lower predicted ground motions at moderate distances (roughly 20-
149 100km) from these models compared to Boore and Atkinson (2008). Boore and Atkinson (2008) note
150 that their distance dependence for small earthquakes and long periods may be biased towards a decay
151 that is less rapid than the true decay. The faster decay of ground motions in Italy (from where a
152 considerable portion of the data used to develop the RESORCE models comes) than in California was
153 previously noted by Scasserra *et al.* (2009).

154 4. Magnitude scaling

155 The magnitude scaling of the five models show the expected behaviour of higher scaling at long
156 structural periods (Figure 3). All models show nonlinear magnitude scaling with, generally, lower

¹² The expression ‘anelastic attenuation’ is only strictly valid for GMPEs for Fourier amplitudes and not response spectral ordinates.

157 dependence of ground motions on magnitude for large events. This nonlinear behaviour is expected
158 from physical models (e.g. Douglas and Jousset, 2011). Some studies (e.g. Schmedes and Archuleta,
159 2008) provide physical arguments for oversaturation of short-period ground motions for large
160 earthquakes (i.e. ground motions that decrease as magnitude increases). This effect is not seen for any
161 of the final RESORCE models for magnitudes within their range of applicability. However, when
162 Akkar *et al.* (2013a, b) included a cubic magnitude term they found that the obtained model predicted
163 oversaturation for $M_w > 7.25$, which they considered physically unrealistic and hence they finally
164 adopted a functional form that did not allow such oversaturation. They note, however, that due to a
165 lack of data from large earthquakes in Europe and the Middle East there is considerable epistemic
166 uncertainty in magnitude scaling for $M_w > 7.5$ and hence they suggest including additional branches in a
167 logic tree to account for this uncertainty. As for the distance decay, within the magnitude range that is
168 well covered by data (M_w 5 to 7) the models predict similar spectral accelerations whereas for larger
169 earthquakes the models differ greatly, depending on whether they are solely driven by the data or the
170 functional form assumed. The magnitude scaling of the RESORCE models is broadly in line with that
171 predicted by the Boore and Atkinson (2008) GMPEs, although because of the lower attenuation
172 predicted by this model there is a considerable offset in the predictions at the considered distance of
173 30km.

174 5. Style-of-faulting factors

175 The effect of style of faulting (faulting mechanism) on strong ground motion was highlighted by the
176 review of Bommer *et al.* (2003), who compared predictions of the reverse-to-strike-slip spectral ratios
177 ($F_{R,SS}$) for various GMPEs (their Figure 3) and who also discussed the limited number of estimates of
178 the ratio of normal-to-strike-slip motions ($F_{N,SS}$) then available. In the decade since then many more
179 estimates of these factors have been published as part of GMPEs, including in the NGA models, but
180 they still show considerable dispersion. Nevertheless, as shown by the example of the Boore and
181 Atkinson (2008) ratios plotted on Figure 4, reverse-faulting events are often thought to generate
182 slightly higher amplitude motions than strike-slip earthquakes that in turn are slightly higher than
183 motions from normal-faulting earthquakes.

184 Figure 4 compares $F_{R,SS}$ and $F_{N,SS}$ for the five RESORCE models [and those of Boore and Atkinson
185 (2008)]. All developers, except Hermkes *et al.* (2013), assumed ratios that are independent of
186 magnitude and distance. Using a nonparametric approach Hermkes *et al.* (2013) find ratios that depend
187 weakly on these variables. These ratios are generally quite close to unity (i.e. rupture mechanism has
188 no effect on spectral accelerations) but two models (Bindi *et al.*, 2013; Hermkes *et al.*, 2013) show
189 large values for $F_{R,SS}$ (>1.25), particularly those of Hermkes *et al.* (2013), whose ratios reach over two.
190 $F_{N,SS}$ are generally within 0.1 of unity except, again, for Hermkes *et al.* (2013) at moderate and long
191 periods where the ratios reach 1.5. The overall observation that the style of faulting has a limited

192 impact on spectral accelerations is in line with the findings from previous studies, including those
193 associated with the NGA models. The usual order of which style of faulting leads to the highest and
194 lowest motions is reversed in the model of Derras *et al.* (2013), which predicts that normal-faulting
195 events cause higher SAs than reverse-faulting earthquakes. One possible reason for this is that only 93
196 of the 1,088 records used to derive this model are from reverse-faulting events (compared to 540 from
197 normal and 455 from strike-slip earthquakes) and, in addition, each earthquake is only associated with
198 on average 3.4 records (Table 1) and hence the style-of-faulting factors are poorly constrained. In view
199 of this, the style-of-faulting factors implied by the model of Derras *et al.* (2013) are not recommended
200 for application. Compared with the NGA database, RESORCE is much richer in data from normal-
201 faulting earthquakes, e.g. less than 3% of the records used by Boore and Atkinson (2008) come from
202 normal events, and consequently the estimates of $F_{N,SS}$ from the RESORCE models are much better
203 constrained.

204 6. *Scaling with V_{S30}*

205 All models (Figure 5) predict an overall inverse dependence on V_{S30} , i.e. as V_{S30} increases ground
206 motions decrease, even if no functional form was imposed. In addition, the models predict a stronger
207 dependence on V_{S30} for longer structural periods (Figure 5, Figure 6). All of the models except those
208 of Bindi *et al.* (2013) and Bora *et al.* (2013) include nonlinear site behaviour, i.e. lower amplifications
209 on soft soils (low V_{S30}) for stronger shaking (Figure 5, Figure 6). However, once again the dispersion
210 in the predictions is quite large, particularly at longer periods.

211 The ratios of spectral accelerations on soft soil to rock reach their peak for a structural period of
212 around 1s with ratios of three or even higher (up to about 5.5 for Hermkes *et al.*, 2013) (Figure 6),
213 although they show considerable variation among models. Similarly the peak in the stiff-soil-to-rock
214 ratios is at about 1s but the peak ratios are lower (around 1.5) and show smaller dispersion. These
215 ratios are similar to those represented in a similar plot (their Figure 10) by Ambraseys *et al.* (2005).
216 One difference with the NGA models, however, is that the peak amplification occurs in the NGA
217 models at a longer period ($>3s$) [see, e.g., the curves for Boore and Atkinson (2008) in Figure 6],
218 which could be related to soil profiles that are deeper on average in California than in Europe and the
219 Middle East (Stewart *et al.*, 2012) or to smaller sedimentary basins in Europe compared to California
220 that give rise to 2D-3D basin effects at shorter periods. Also the long-period site amplifications
221 predicted by the Boore and Atkinson (2008) model are generally lower than those predicted by the
222 RESORCE models.

223 7. *Predicted response spectra*

224 The models all predict similar response spectra on NEHRP B/C boundary sites for M_w 5 to 7 at
225 $R_{JB}=10km$ (Figure 7); any differences in the models become apparent at large magnitudes, longer

226 distances and for softer sites (see, e.g., Figures 1 and 2). For the largest events, the functional forms
227 used to develop the models of Akkar *et al.* (2013a, b), Bindi *et al.* (2013), Bora *et al.* (2013) and
228 Hermkes *et al.* (2013) allow evaluation up to M_w 8 whereas the model of (Derras *et al.* (2013) should
229 not be used for such magnitudes. The periods of the plateaus in the spectra do not show strong
230 magnitude dependency. Predictions from the GMPEs of Boore and Atkinson (2008) at this distance
231 for all magnitudes fall roughly in the middle of the predictions from the RESORCE models but
232 because of the lower attenuation predicted by this model the predicted spectra for longer distances are
233 higher than those predicted by the RESORCE models (not shown here).

234 The predicted spectra for soft soil sites show a much broader plateau and greater dispersion than in the
235 predicted spectra on rock (Figure 8), which is due to the strong long-period site amplifications
236 predicted by some models (Figure 6). Again a factor of two in the predicted spectral accelerations can
237 be seen between the highest and lowest predictions.

238 8. Aleatory variability

239 As noted above, all models predict homoscedastic aleatory variability (standard deviation, sigma) and
240 consequently only a single figure is required to summarise this aspect of the models (Figure 9). As
241 Akkar *et al.* (2013a, b) note there is limited data from larger earthquakes and consequently the
242 apparent magnitude dependency seen within their between-event residuals may not represent the true
243 aleatory variability at large magnitudes. Consequently they assumed magnitude-independent sigmas.
244 Similar arguments hold for the other models. The sigmas fall into two groups: Bora *et al.* (2013),
245 which has slightly higher values, and the other four models. This difference is related to higher values
246 of the between-event (tau) standard deviations whilst the within-event (phi) standard deviations are
247 similar. The sigmas show similar dependence on period with a first peak between 0.1 and 0.2s (near
248 the plateau of predicted response spectra) and then a further increase in sigma as period increases.
249 However, the period dependency is quite limited with less than a 20% difference between the lowest
250 and the highest sigma.

251 The values of tau for the models of Akkar *et al.* (2013a, b), Derras *et al.* (2013) and Hermkes *et al.*
252 (2013) are similar to those of the NGA models although slightly higher [see, e.g., the curve for Boore
253 and Atkinson (2008) shown on Figure 9], whereas the taus of Bindi *et al.* (2013) and Bora *et al.* (2013)
254 are larger. The values of phi of the different models are slightly (by about 0.1 ln units for moderate
255 magnitudes) higher than those of the NGA models [again, see the curve for Boore and Atkinson
256 (2008) on Figure 9], which leads to overall sigmas that are also about 0.1 ln units higher. The NGA
257 models of aleatory variability also do not show a strong period dependence. The higher estimates of
258 aleatory variability for the RESORCE models compared with the sigmas of the NGA models could be
259 related to: a) truly higher variability in ground-motion databases in Europe and the Middle East
260 (caused by, e.g., mixing together of data from a wide geographical region with different tectonics and

261 geology); b) the use of more data from small earthquakes whose motions are possibly intrinsically
262 more variable than those from large events because of, e.g., higher variability in stress drops; or c)
263 problems with the metadata in RESORCE, particularly for small events (or more likely a mixture of
264 these reasons). (Insufficiently complex functional forms for the RESORCE models cannot explain this
265 difference because it is apparent even for the non-parametric models). One aspect of the metadata that
266 could be revisited in future models for Europe and the Middle East, particularly for applications below
267 M_w 5.5, is the use of moment magnitude (sometimes obtained by conversions from other magnitude
268 scales) rather than local magnitude (M_L) for the smaller earthquakes. It was shown by Bindi *et al.*
269 (2007), for north-western Turkey, that the use of M_L for small earthquakes leads to lower estimates of
270 between-event variability (τ) compared to using M_w . This is because corner frequencies for such
271 earthquakes are generally higher than 1Hz, which is the frequency range at which M_L is measured
272 whereas M_w is measuring energy at frequencies below the corner and hence it is a poorer measure of
273 the size of such events. Therefore, it could be envisaged that M_L is used below, say, M_w 5.5 for the
274 derivation of GMPEs and then in applications the local magnitude scale for that region is used to
275 evaluate the model. Sabetta and Pugliese (1987) adopted a similar composite magnitude scale (M_L
276 below M 5.5 and surface-wave magnitude, M_s , above this limit) when deriving their GMPEs for Italy.

277 9. Conclusions

278 In this article, various aspects of the five ground-motion models that are described in other articles in
279 this special issue have been compared. Despite all the developers having started with the same
280 common strong-motion archive and having used the same independent parameters, the predicted
281 spectral accelerations from the models show significant differences, which can be related to varying
282 data selection criteria and derivation techniques. All aspects of the models for the median ground
283 motions (magnitude scaling, style-of-faulting factors, distance decay and site amplification) show
284 variation from one model to the next. These differences when combined lead to variations in the
285 predicted response spectral accelerations for scenarios of interest of more than a factor of two. These
286 differences demonstrate that epistemic uncertainty in ground-motion prediction in Europe and the
287 Middle East remains large and it cannot be explained by differences in the metadata of the strong-
288 motion records used or different sets of independent parameters (e.g. hypocentral distance rather than
289 Joyner-Boore distance or surface-wave magnitude rather than moment magnitude). One of the reasons
290 for this large epistemic uncertainty is that a given earthquake in Europe and the Middle East is, on
291 average, recorded by fewer strong-motion instruments than in California, Taiwan and Japan and hence
292 the aspects of the models related to source effects are less well constrained.

293 The aleatory variabilities are slightly higher than those associated with the NGA models, again (e.g.
294 Strasser *et al.*, 2009) showing that this aspect of ground-motion modelling is stable within a narrow
295 band (± 0.2 ln units) around 0.7 (for PGA). In particular, estimates of the within-event variability (ϕ)

296 show little variation from one study to the next. The between-event variability (τ), however, can be
297 significantly affected by the inclusion of data from smaller (less well-studied) earthquakes. Further
298 studies to constrain the value of τ for European events are, therefore, recommended.

299 The five models presented in this volume should be of considerable value for seismic hazard
300 assessments in Europe and the Middle East, providing both state-of-the-art predictions of spectral
301 accelerations and a basis for quantifying epistemic uncertainty in those predictions.

302 *Acknowledgements*

303 The work presented in this article was partially funded by the SHARE (Seismic Hazard Harmonization
304 in Europe) Project funded under contract 226967 of the EC-Research Framework Programme FP7 and
305 by the task ‘Reference database for seismic ground motion in Europe’ of the SIGMA (Seismic Ground
306 Motion Assessment) project. We thank the personnel of the organisations operating seismological
307 stations and freely disseminating their ground-motion data and related metadata, without which the
308 derivation of the ground-motion models compared here would have been impossible. Finally, we
309 thank an anonymous reviewer for their constructive comments on a previous version of this article.

310 *References*

311 Abrahamson, N. A., Youngs, R. R. (1992), A stable algorithm for regression analyses using the
312 random effects model, *Bulletin of the Seismological Society of America*, 82(1), 505-510.

313 Abrahamson, N., Atkinson, G., Boore, D., Bozorgnia, Y., Campbell, K., Chiou, B., Idriss, I. M., Silva,
314 W., Youngs, R. (2008), Comparisons of the NGA ground-motion relations, *Earthquake Spectra*, 24(1),
315 45-66, doi: 10.1193/1.2924363.

316 Akkar, S., Sandikkaya, M. A., Bommer, J. J. (2013a), Empirical ground-motion models for point- and
317 extended-source crustal earthquake scenarios in Europe and the Middle East, *Bulletin of Earthquake*
318 *Engineering*, this issue, doi: 10.1007/s10518-013-9461-4.

319 Akkar, S., Sandikkaya, M. A., Bommer, J. J. (2013b), Erratum: Empirical ground-motion models for
320 point- and extended-source crustal earthquake scenarios in Europe and the Middle East, *Bulletin of*
321 *Earthquake Engineering*, this issue.

322 Akkar, S., Sandikkaya, M. A., Şenyurt, M., Azari, A. S., Ay, B. Ö., Traversa, P., Douglas, J., Cotton,
323 F., Luzi, L., Hernandez, B., Godey, S. (2013c), Reference database for seismic ground-motion in
324 Europe (RESORCE), *Bulletin of Earthquake Engineering*, this issue, doi: 10.1007/s10518-013-9506-8.

325 Ambraseys, N. N., Douglas, J., Sarma, S. K., Smit, P. M. (2005), Equations for the estimation of
326 strong ground motions from shallow crustal earthquakes using data from Europe and the Middle East:

327 Horizontal peak ground acceleration and spectral acceleration, *Bulletin of Earthquake Engineering*,
328 3(1), 1-53, doi: 10.1007/s10518-005-0183-0.

329 Bindi, D., Massa, M., Luzi, L., Ameri, G., Pacor, F., Puglia, R., Augliera, P. (2013), Pan-European
330 ground-motion prediction equations for the average horizontal component of PGA, PGV, and 5%-
331 Damped PSA at spectral periods up to 3.0 s using the RESORCE dataset, *Bulletin of Earthquake*
332 *Engineering*, submitted to this issue.

333 Bindi, D., Parolai, S., Grosser, H., Milkereit, C., Durukal, E. (2007), Empirical ground-motion
334 prediction equations for northwestern Turkey using the aftershocks of the 1999 Kocaeli earthquake.
335 *Geophysical Research Letters*, 34(L08305).

336 Bommer, J. J., Douglas, J., Strasser, F. O. (2003), Style-of-faulting in ground-motion prediction
337 equations, *Bulletin of Earthquake Engineering*, 1(2), 171-203.

338 Bommer, J. J., Scherbaum, F., Bungum, H., Cotton, F., Sabetta, F., Abrahamson, N. A. (2005), On the
339 use of logic trees for ground-motion prediction equations in seismic-hazard analysis, *Bulletin of the*
340 *Seismological Society of America*, 95(2), 377-389, doi: 10.1785/0120040073.

341 Boore, D. M., Atkinson, G. M. (2008), Ground-motion prediction equations for the average horizontal
342 component of PGA, PGV, and 5%-damped PSA at spectral periods between 0.01s and 10.0s,
343 *Earthquake Spectra*, 24(1), 99-138.

344 Bora, S. S., Scherbaum, F., Stafford, P. J., Kuehn, N. (2013), Fourier spectral- and duration models for
345 the generation of response spectra adjustable to different source-, propagation-, and site conditions,
346 *Bulletin of Earthquake Engineering*, this issue, doi: 10.1007/s10518-013-9482-z.

347 Building Seismic Safety Council (2009), 2009 NEHRP Recommended Seismic Provisions For New
348 Buildings and Other Structures: Part 1, Provisions, Federal Emergency Management Agency (P-750),
349 Washington D.C.

350 Castellaro, S., Mulargia, F., Rossi, P. L. (2008), V_{S30} : Proxy for seismic amplification? *Seismological*
351 *Research Letters*, 79(4), 540–543, doi: 10.1785/gssrl.79.4.540.

352 Chiou, B., Darragh, R., Gregor, N., Silva, W. (2008), NGA project strong-motion database,
353 *Earthquake Spectra*, 24(1), 23-44, doi: 10.1193/1.2894831.

354 Derras, B., Cotton, F., Bard, P.-Y. (2013), Towards fully data driven ground-motion prediction models
355 for Europe, *Bulletin of Earthquake Engineering*, this issue, doi: 10.1007/s10518-013-9481-0.

356 Douglas, J. (2010), Consistency of ground-motion predictions from the past four decades, *Bulletin of*
357 *Earthquake Engineering*, 8(6), 1515-1526, doi: 10.1007/s10518-010-9195-5.

358 Douglas, J., Halldórsson, B. (2010), On the use of aftershocks when deriving ground-motion
359 prediction equations, 9th US National and 10th Canadian Conference on Earthquake Engineering:
360 Reaching Beyond Borders, paper ID 220.

361 Douglas, J., Jousset, P. (2011), Modeling the difference in ground-motion magnitude-scaling in small
362 and large earthquakes, *Seismological Research Letters*, 82(4), 504-508, doi: 10.1785/gssrl.82.4.504.

363 Hermkes, M., Kuehn, N. M., Riggelsen, C. (2013), Simultaneous quantification of epistemic and
364 aleatory uncertainty in GMPEs using Gaussian process regression, *Bulletin of Earthquake*
365 *Engineering*, this issue, doi: .

366 Petersen, M. D., Frankel, A. D., Harmsen, S. C., Mueller, C. S., Haller, K. M., Wheeler, R. L.,
367 Wesson, R. L., Zeng, Y., Boyd, O. S., Perkins, D. M., Luco, N., Field, E. H., Wills, C. J., Rukstales,
368 K. S. (2008), Documentation for the 2008 Update of the United States National Seismic Hazard Maps,
369 Open-File Report 2008-1128, U.S. Department of the Interior, U.S. Geological Survey, 61 pp.

370 Power, M., Chiou, B., Abrahamson, B., Bozorgnia, Y., Shantz, T., Roblee, C. (2008), An overview of
371 the NGA project, *Earthquake Spectra*, 24(1), 3-21, doi: 10.1193/1.2894833.

372 Sabetta, F., Pugliese, A. (1987), Attenuation of peak horizontal acceleration and velocity from Italian
373 strong-motion records, *Bulletin of the Seismological Society of America*, 77(5), 1491–1513.

374 Scasserra, G., Stewart, J.P., Bazzurro, P., Lanzo, G., Mollaioli, F. (2009), A comparison of NGA
375 ground-motion prediction equations to Italian data, *Bulletin of the Seismological Society of America*,
376 99(5), 2961-2978.

377 Schmedes, J., Archuleta, R. J. (2008), Near-source ground motion along strike-slip faults: Insights into
378 magnitude saturation of PGV and PGA, *Bulletin of the Seismological Society of America*, 98(5),
379 2278-2290, doi: 10.1785/0120070209.

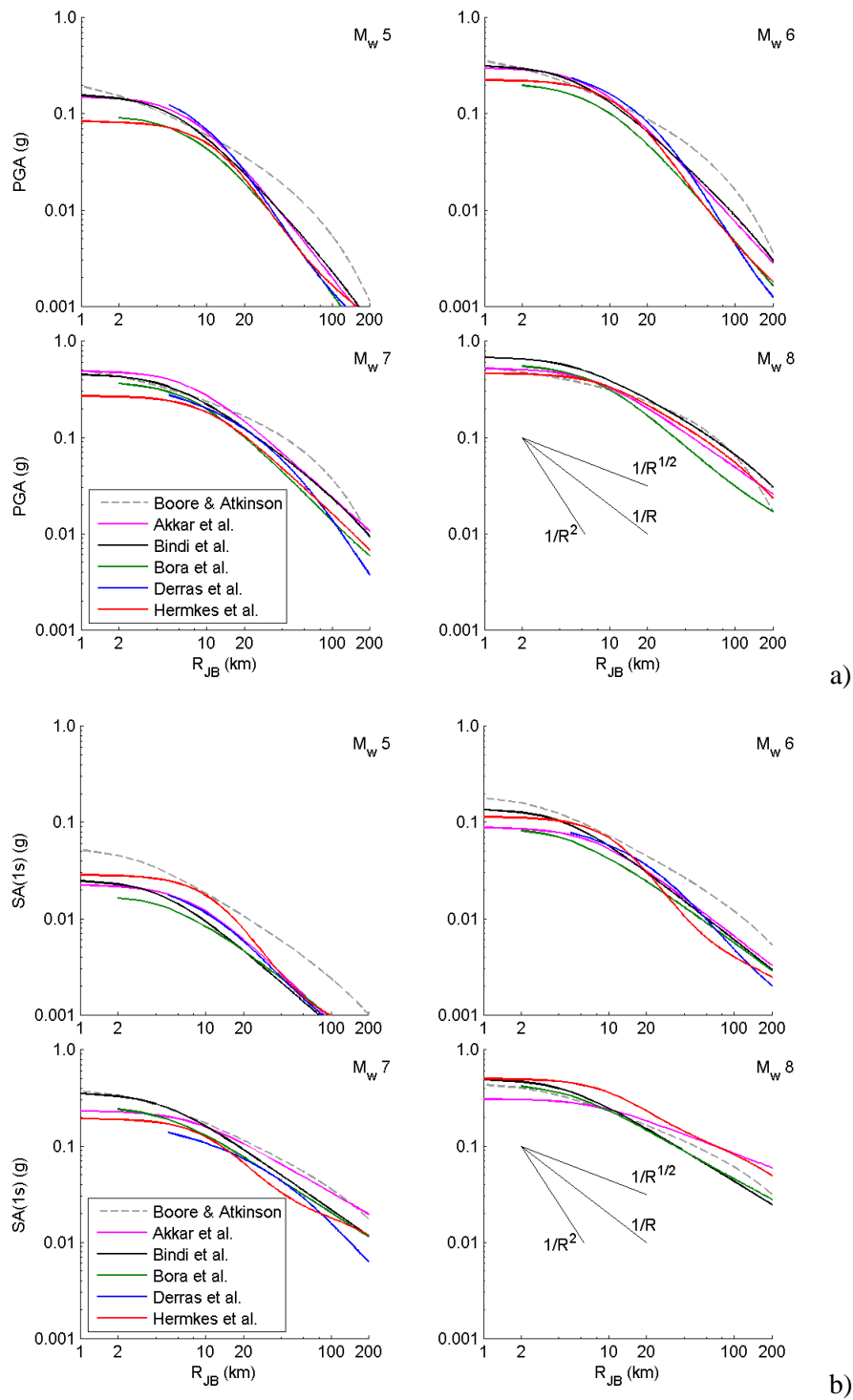
380 Stafford, P. J., Strasser, F. O., Bommer, J. J. (2008), An evaluation of the applicability of the NGA
381 models to ground-motion prediction in the Euro-Mediterranean region, *Bulletin of Earthquake*
382 *Engineering*, 6(2), 149–177.

383 Stewart, J.P., Douglas, J., Javanbarg, M. B., Di Alessandro, C., Bozorgnia, Y., Abrahamson, N. A.,
384 Boore, D. M., Campbell, K. W., Delavaud, E., Erdik, M., Stafford, P. J. (2012), Selection of a global
385 set of ground motion prediction equations: Work undertaken as part of Task 3 of the GEM-PEER
386 Global GMPEs project, PEER Report 2012/xx, Pacific Earthquake Engineering Research Center.

387 Strasser, F., Abrahamson, N.A., Bommer, J.J. (2009), Sigma: issues, insights, and challenges,
388 *Seismological Research Letters*, 80(1), 40-56.

389 USNRC (2012). Practical Implementation Guidelines for SSHAC Level 3 and 4 Hazard Studies.
390 NUREG-2117, US Nuclear Regulatory Commission, Washington, DC.

391

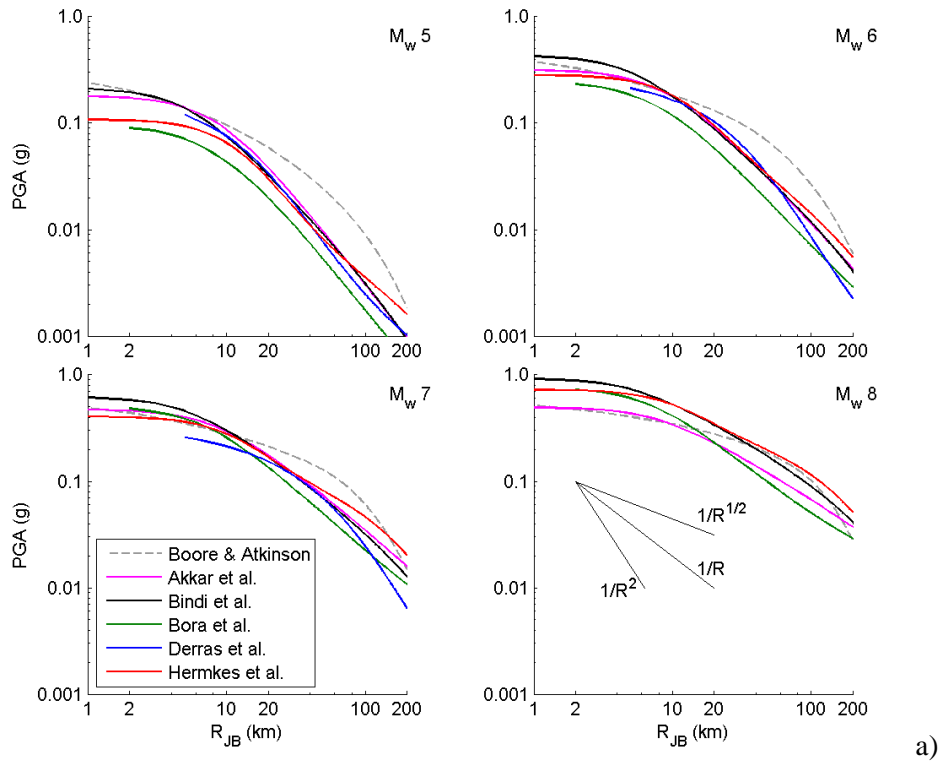


393

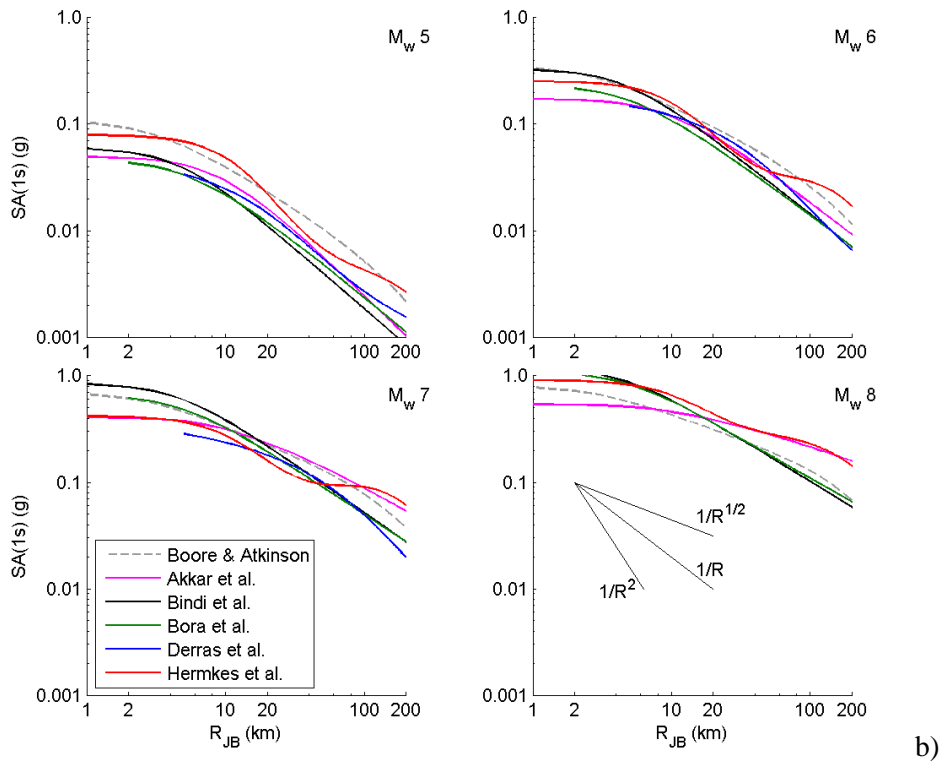
394

395 *Figure 1: Comparison of distance scaling for strike-slip earthquakes for $V_{S30}=760$ m/s (NEHRP B/C*
 396 *boundary) for M_w 5 (top left), 6 (top right), 7 (bottom left) and 8 (bottom right) for a) PGA and b)*
 397 *SA(1s). The predictions from the model of Derras et al. (2013) are not shown for M_w 8 since this is*
 398 *outside its range of applicability. The other models are shown for this magnitude even though some*
 399 *developers do not recommend their application for such large events.*

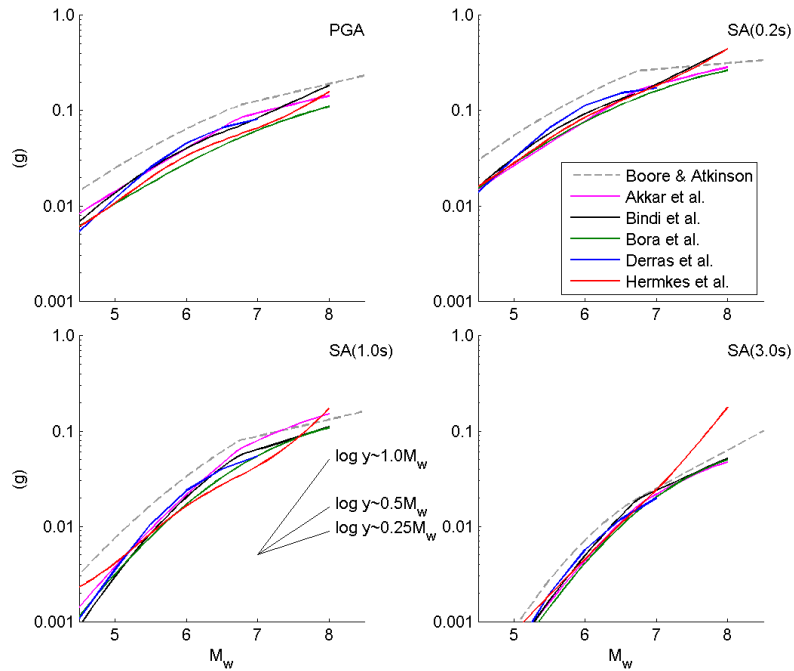
400



401

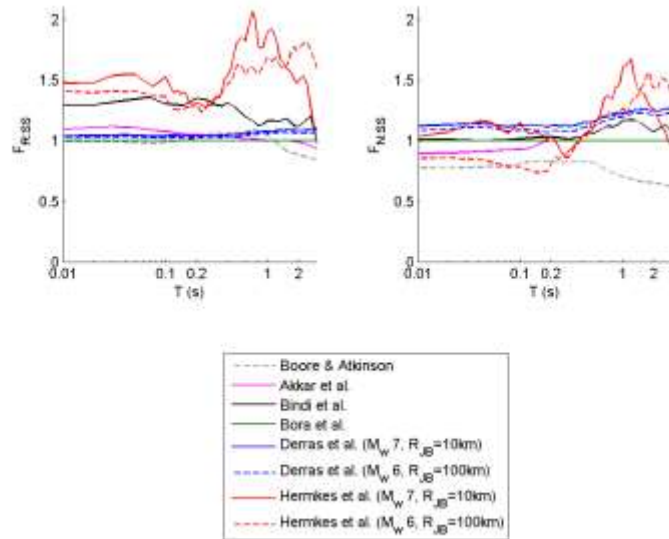


402 *Figure 2: Comparison of distance scaling for strike-slip earthquakes for $V_{S30}=270$ m/s (NEHRP D) for*
 403 *M_w 5 (top left), 6 (top right), 7 (bottom left) and 8 (bottom right) for a) PGA and b) SA(1s). The*
 404 *predictions from the model of Derras et al. (2013) are not shown for M_w 8 since this is outside its*
 405 *range of applicability. The other models are shown for this magnitude even though some developers*
 406 *do not recommend their application for such large events.*



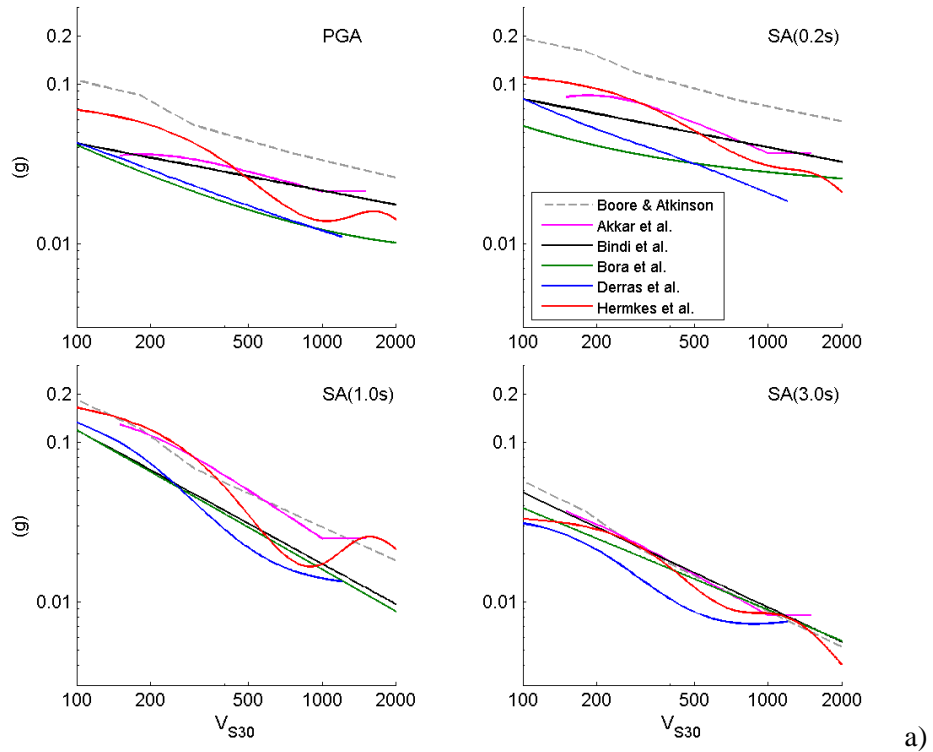
407

408 *Figure 3: Comparison of magnitude scaling of the median ground motion for strike-slip earthquakes*
 409 *and $V_{S30}=760$ m/s (NEHRP B/C boundary) at $R_{JB}=30$ km for PGA (top left), SA(0.2s) (top right),*
 410 *SA(1.0s) (bottom left) and SA(3.0s) (bottom right). Predictions are generally shown up to M_w 8 even*
 411 *though some developers do not recommend their models for such large events.*

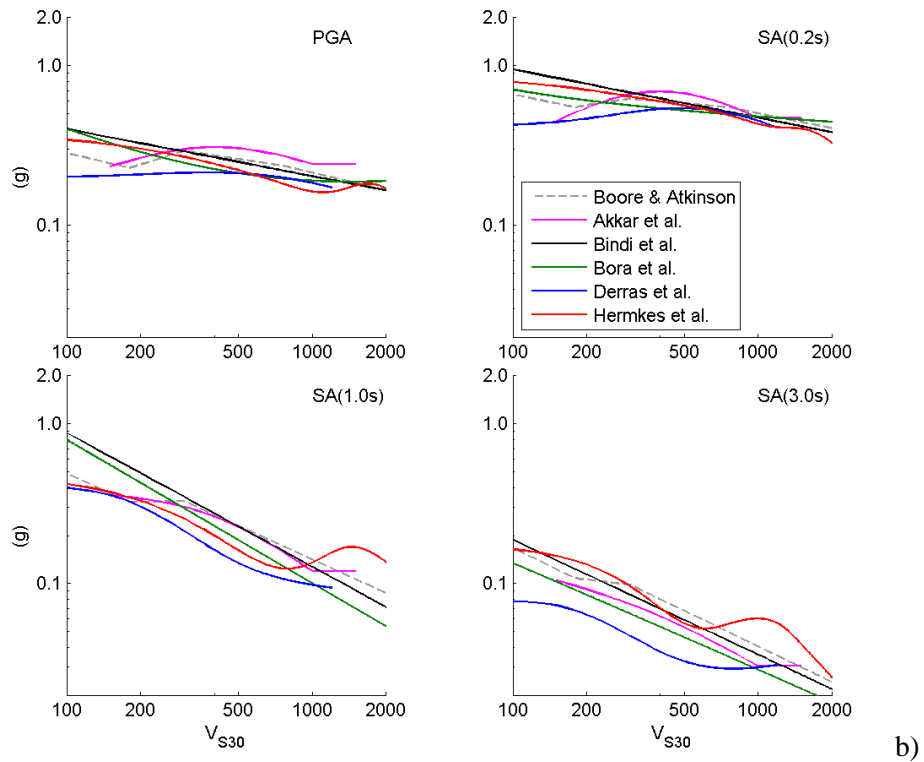


412

413 *Figure 4: Comparison of style-of-faulting factors for SA: a) ratio of reverse to strike-slip ($F_{R,SS}$) and b)*
 414 *ratio of normal to strike-slip ($F_{N,SS}$). Ratios are scenario-independent except for those of Hermkes et*
 415 *al. (2013). The predictions of Bora et al. (2013) are independent of the style of faulting. $F_{N,SS}$ of Akkar*
 416 *et al. equals unity for $T>0.2$ s and therefore this curve is under that of Bora et al. (2013) for these*
 417 *periods.*

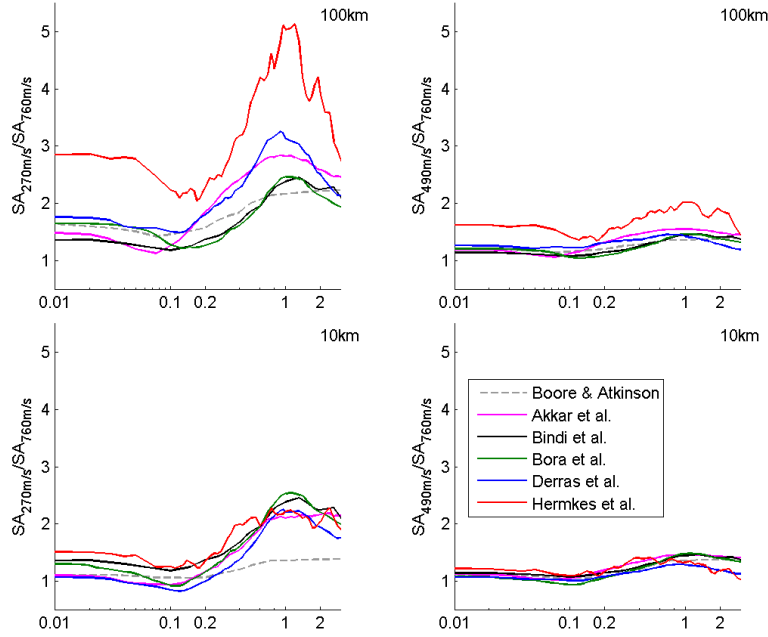


418



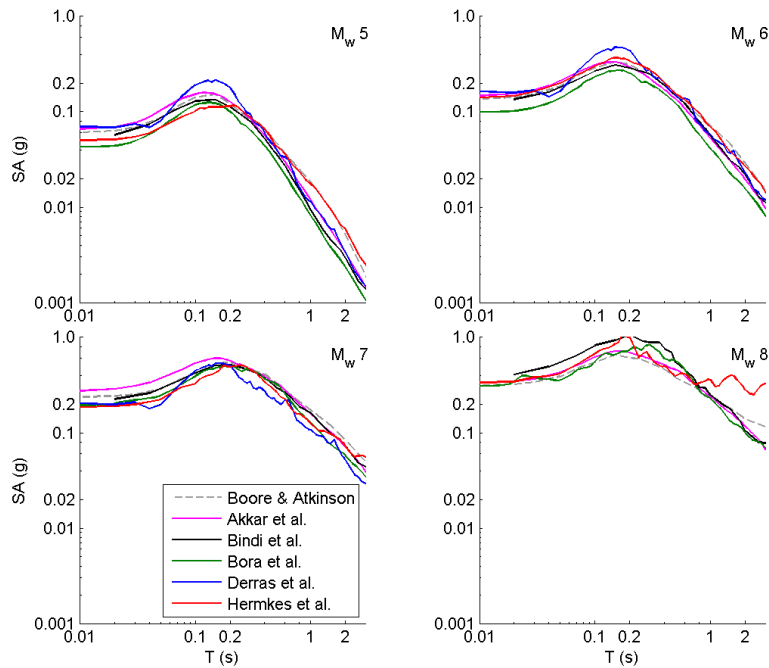
419

420 *Figure 5 Comparison of V_{S30} scaling of the median ground motion for M_w 7 strike-slip earthquakes for*
 421 *PGA (top left), SA(0.2s) (top right), SA(1.0s) (bottom left) and SA(3.0s) (bottom right) at:*
 422 *a) $R_{JB} = 100$ km and b) $R_{JB} = 10$ km.*



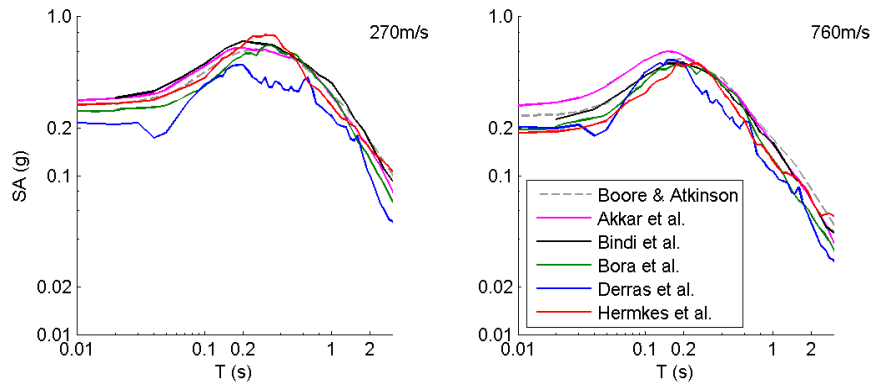
423

424 *Figure 6: Comparison of ratios between SA for $V_{S30}=270\text{m/s}$ (NEHRP D) (left) and SA for*
 425 *$V_{S30}=490\text{m/s}$ (NEHRP C) (right) to SA for $V_{S30}=760\text{m/s}$ for M_w 7 (strike-slip) at $R_{JB}=100\text{km}$ (top) and*
 426 *M_w 7 (strike-slip) at $R_{JB}=10\text{km}$ (bottom).*



427

428 *Figure 7: Comparison of median 5% damped spectra for strike-slip earthquakes and $V_{S30}=760\text{ m/s}$*
 429 *(NEHRP B/C boundary) at $R_{JB}=10\text{ km}$ for M_w 5 (top left), 6 (top right), 7 (bottom left) and 8 (bottom*
 430 *right). The predictions from the model of Derras et al. (2013) are not shown for M_w 8 since this is*
 431 *outside its range of applicability. The other models are shown for this magnitude even though some*
 432 *developers do not recommend their application for such large events.*



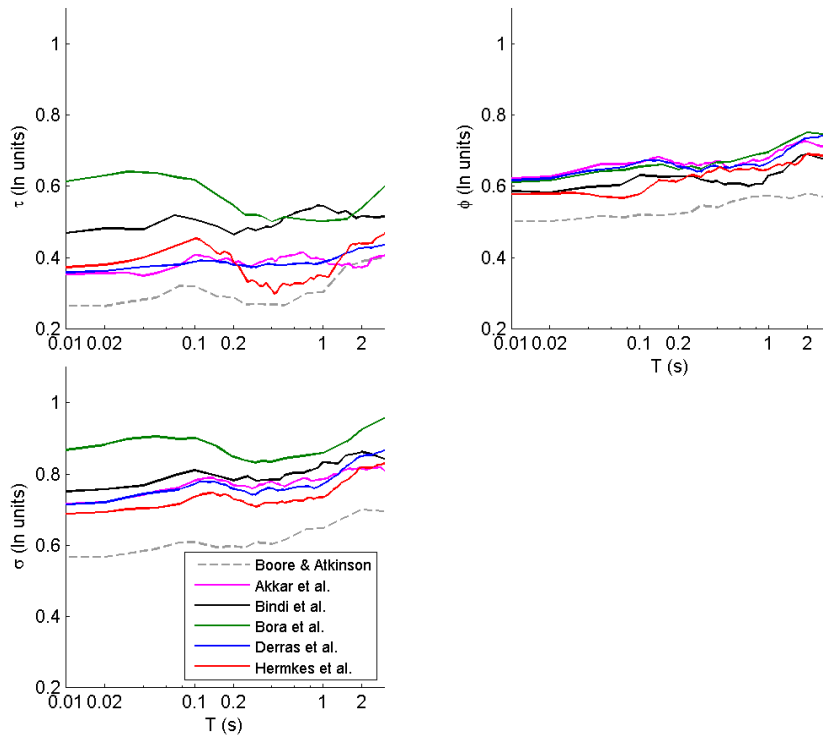
433

434

a)

b)

435 Figure 8: Comparison of median 5% damped spectra for strike-slip earthquakes at $R_{JB}=10$ km for
 436 M_w 7 and a) $V_{S30}=270$ m/s (NEHRP D) and b) $V_{S30}=760$ m/s (NEHRP B/C boundary).



437

438 Figure 9: Comparison of the between-event (τ), within-event (ϕ) and total (σ) standard
 439 deviations. All models have homoscedastic standard deviations.

440

441 Table 1: Number of different earthquakes, stations and records used to derive the five models,
 442 magnitude and distance ranges of the data used, the ranges of applicability recommended by the model
 443 developers and the exclusion criteria used to select the records used to derive the model.

Model	Akkar et al.	Bindi et al. (V_{S30} model)	Bora et al.	Derras et al.	Hermkes et al.
Number of earthquakes (E)	221	225	369	320	279
Number of stations (S)	322	345	341	201	251
Number of records (R)	1041	1224	1232	1088	835
R/E	4.7	4.8	3.3	3.4	3.0
M_{\min} to M_{\max} (data used)	4.0 to 7.6	4.0 to 7.6	4.0 to 7.6	3.6 to 7.6	4.0 to 7.6
M_{\min} to M_{\max} (recommended)	4.0 to 8.0	4.0 to 7.6	4.0 to 7.6	4.0 to 7.0	4.0 to 7.6
R_{\min} to R_{\max} (km) (data used)	0 to 200	0 to 300	0 to 200	0 to 547km	0 to 200
R_{\min} to R_{\max} (km) (recommended)	0 to 200	0 to 300	0 to 200	5 to 200km	0 to 200
Record exclusion criteria (other than in terms of magnitude and distance)	Singly-recorded earthquakes; all three components not available; focal depth greater than 30km; sites with no measured V_{S30} ; structural period beyond usable period range defined by Akkar and Bommer (2006); events with $M_w < 5$ with fewer than 3 records; unknown or oblique style of faulting; not free-field.	Unknown style of faulting; sites with no measured V_{S30} ; singly-recorded earthquakes; only records with low-pass cut-off frequency lower than 20Hz and outside passband of high-pass filter all three components not available; focal depth > 35km.	Not representative of shallow crustal event; unknown style of faulting; only one horizontal component; sites with no measured V_{S30} ; poor quality record; high-pass cut-off frequency higher than Brune-source corner frequency for stress drop of 100bars.	Focal depth more than 25km; sites with no measured V_{S30} ; unknown style of faulting	Unknown style of faulting; sites with no measured V_{S30} ; not free-field conditions; high-pass cut-off frequency higher than 0.25Hz

444